Flow-Induced Vibration Analysis of Supported Pipes with a Crack

Jin-Hyuk Lee[1]*, Samer Masoud Al-Said[2,3]
[1]Department of Mechanical Engineering, American University of Sharjah, Sharjah, UAE, [2]Department of Mechanical Engineering, Jordan University of Science and Technology, Irbid, Jordan, [3]visiting professor at Department of Mechanical Engineering, American University of Sharjah, Sharjah, UAE
*Corresponding author: Department of Mechanical Engineering, American University of Sharjah, PO Box 26666, Sharjah, UAE, jinhyuk@aus.edu

Abstract: In this paper, the effect of a crack to the flow-induced vibration characteristics of supported pipes is investigated based on vibration method. In order to estimate the crack location and depth in the pipe, we need to utilize the variation of the difference between the natural frequencies of the pipe conveying fluid with and without crack. The pipe is fluid loaded via interaction with the fluid. Fluid loading has two main effects on vibrating pipes: first, the fluid mass loads the pipe, meaning that the pipe's natural frequencies are altered due to added mass. Secondly, viscous loading is provided to the pipe near the wall due to shear force between the pipe and the fluid. In COMSOL Multiphysics® Module, the Aeroacoustics and Structural physics have been used for frequency domain analysis. Fully developed laminar flow profile is used to simulate the fluid flow inside a pipe. Perfectly Matched layer is used to simulate the unbounded boundary to purely capture the fluid and the pipe system without standing waves; hence the mode shapes are expected to remain unchanged for pipes conveying fluid form ones attained from pipes alone.

Keywords: aeroacoustic, crack, fluid-flow, natural frequency, vibration

1. Introduction

Flow-induce vibration analysis of pipes conveying fluid had gained its attention as the pipes are widely used in many industrial areas such as skyscraper cooling systems, petrol and gas transportation systems. Over the past decades, many studies have been conducted on the dynamic characteristics of pipeline systems subject to different loading conditions [1-3]. These pipes working hard on our mundane life would be cracked as a result of various loads while conveying fluid, which could lead catastrophic event if not prevented. Hence, analyzing the vibrational behavior of the cracked pipes would be practically important. Previously the crack identification algorithm for a beam has been developed and verified against the experimental as well as finite element (FE) analysis results [4-7]. However, published work of the vibrational study on the cracked pipes conveying fluid flow is rather scarce.

In this paper the vibrational behavior of the pipe conveying fluid flow with cracks is numerically investigated based on vibration method. Simulated results will be used to help to model the similar system mathematically.

2. Flow-Induced Pipe with Crack Model

In this section an overall mathematical model describing vibration behavior of a cracked fluid-conveying pipe. The cracked beam can be modeled as two uniform Euler-Bernoulli beams connected by a massless torsional spring to consider rotational discontinuity in beam's deflection at the crack location. In order to combine global effects of crack and vibration characteristics, the assumed mode method and the Lagrange method are used [4].

The kinetic energy of the beam is obtained as follows:

$$T_{pipe} = \frac{1}{2} m \left\{ \int_0^{x_c} \left(\frac{\partial y_1(x,t)}{\partial t} \right)^2 dx + \int_{x_c}^{L} \left(\frac{\partial y_2(x,t)}{\partial t} \right)^2 dx \right\} \quad (1)$$

, where T_{pipe} is kinetic energy of the pipe, m is mass per unit length of the pipe, x_c is the distance to the crack location, y is the deflection of the pipe, and L is the total length of the pipe.

$$T_{fluid} = \frac{1}{2} M \left[\int_0^{x_c} \left\{ U^2 + 2U \left(\frac{\partial^2 y_1}{\partial x \partial t} \right) + \left(\frac{\partial y_1}{\partial t} \right)^2 \right\} dx + \int_{x_c}^{L} \left\{ U^2 + 2U \left(\frac{\partial^2 y_2}{\partial x \partial t} \right) + \left(\frac{\partial y_2}{\partial t} \right)^2 \right\} dx \right] \quad (2)$$

, where T_{fluid} is kinetic energy due to fluid inside the pipe, M is mass per unit length of fluid, and

U is fluid velocity. The potential energy of the pipe due to strain energy is

$$V_{pipe} = \frac{1}{2} EI \left\{ \int_0^{x_c} \left(\frac{\partial^2 y_1}{\partial x^2} \right)^2 dx + \int_{x_c}^{L} \left(\frac{\partial^2 y_2}{\partial x^2} \right)^2 dx \right\} + \frac{1}{2} K_R \frac{\partial^2 y_2(x_c)}{\partial x^2} \quad (3)$$

, where E is modulus of elasticity, I is area moment of inertia, K_R is spring coefficient due to crack and y_k (k = 1, 2) represents transverse displacement [8]. The transverse displacement takes the form of a linear combination of admissible function $\phi_{ki}(x)$, and a generalized coordinate $di(t)$ as follows

$$y_k(x,t) = \sum_{i=1}^{n} \phi_{ki}(x) d_i(t) \quad (4)$$

, where the subscript k denotes the number of divided pipes due to crack [8].

Substituting Eq. (1) – Eq. (3) into Lagrange's equation and considering an external forcing term, the equation of motion can be written as:

$$[\mathbf{M}]\ddot{\mathbf{q}} + [\mathbf{K}]\mathbf{q} = \mathbf{F_{ext}} \quad (5)$$

In Eq. (5), the external force term can be assumed to be a viscous drag force due to shear stress inside the pipe wall. It can be replaced with

$$F_{viscous} = \eta A \frac{\Delta \upsilon}{\Delta y} \quad (6)$$

, where A is surface area, Δv is the average fluid velocity, and Δy is separation distance between the wall and the center of the pipe. In Eq. (6), η represents the ratio shown in Eq. (7).

$$\eta = \frac{F/A}{\Delta \upsilon / \Delta y} \quad (7)$$

, where F is a force required to maintain the motion.

Eq. (5) can be reduced to a typical eigenvalue/eigenvector problem which enables us to calculate the analytical values of natural frequencies of the system.

3. Use of COMSOL Multiphysics® Software

The vibrational behavior of a 3D pipe conveying fluid flow is investigated using the commercial finite element software COMSOL Multiphysics®. The 3D model is used based on the Aeroacoustics Module interface with the Structural Mechanics Module. Figure 1 shows a three dimensional finite element (FE) model of a pipe conveying fluid flow.

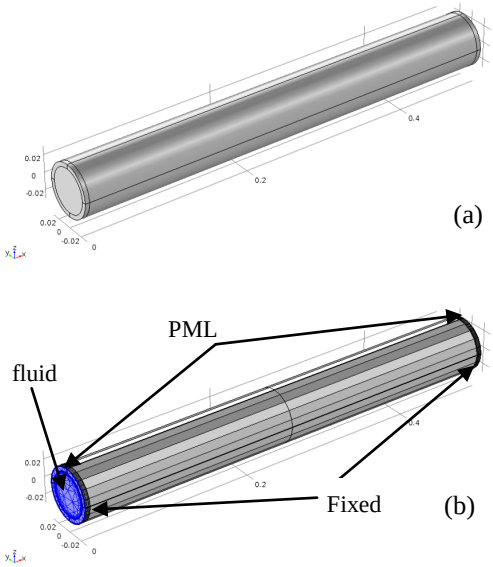

Figure 1. (a) Geometric pipe model, and (b) meshed pipe model without crack where blue colored section represents PML.

Table 1: Structure and material properties of the fluid flow conveying pipe.

	Pipe
Material	Copper
Outer Diameter d	6e-2m
Thickness t	5e-3m
Modulus of Elasticity E	110GPa
Density ρ	8700 kg/m^3
Poisson ratio v	0.35
Pipe length L	0.5m
Beam width w	1.2mm

In order to simulate the flowing fluid inside a pipe, the Linearized Navier-Stokes, Frequency Domain interface is chosen for the study, which solves for the acoustic variations in the pressure, velocity field, and temperature. Coupling the

interfaces to structures enables vibration analysis of the pipe in the presence of flow, such as fluid structure interaction (FSI) in the frequency domain.

The pipe conveying fluid flow is made of copper that is most common type of material due to its quality, safety, and endurance. The fluid type is chosen as water. The material properties of the system are provided in Table 1.

3.1 Governing Equations

The governing equations used to solve for the frequency analysis are the continuity, momentum, and energy equations as follows:

$$\begin{aligned} i\omega\rho + \nabla\cdot(\rho_0 u + \rho u_0) &= M \\ \rho_0(i\omega u + (u\cdot\nabla)u_0 + (u_0\cdot\nabla)u) - \nabla\cdot\sigma &= F \\ \rho_0 C_p(i\omega T + (u\cdot\nabla)T_0 + (u_0\cdot\nabla)T) + \rho C_p(u_0\cdot\nabla)T_0 & \\ -\alpha_0 T_0(i\omega p + (u\cdot\nabla)p_0 + (u_0\cdot\nabla)p) - \alpha_0 T(u_0\cdot\nabla)p_0 & \\ -\nabla\cdot(k\nabla T) &= \Phi + Q \end{aligned} \quad (8)$$

, where p, u, and T are the acoustic perturbations to the pressure, velocity and temperature, respectively [9]. The time derivative of the dependent variables are replaced by $i\omega$ where $\omega = 2\pi f$ which is angular frequency. The stress tensor is σ and Φ is the viscous dissipation function which is set to zero. The right-hand side source term M, F, and Q are mass source, volume force source, and heat source. The default values are all zero for those sources. The variables with a zero subscripts are the background mean flow values. C_p and k denote heat capacity at constant pressure and thermal conductivity, respectively and they are both zero by default. ∇ is the gradient or del operator. The constitutive equations are the stress tensor and the linearized equation of state, while the Fourier heat conduction law is included in the energy equation [9].

$$\begin{aligned} \sigma &= -pI + \mu\left(\nabla u + (\nabla u)^T\right) + \left(\mu_B - \frac{2}{3}\mu\right)(\nabla\cdot u)I \\ \rho &= \rho_0(\beta_T p - \alpha_0 T) \end{aligned} \quad (9)$$

, where μ is dynamic viscosity, μ_B is bulk viscosity, I is the identity tensor, and β_T is the isothermal compressibility [9].

Consider a pipe system, with n degrees of freedom, described by an equation of the form

$$M\ddot{u} + D\dot{u} + Ku = F \quad (10)$$

, where u is the displacement vector, K is the stiffness matrix, D is the damping matrix, and M is the mass matrix. In the frequency domain, Eq. (10) takes the form

$$-\omega^2 M u_0 + i\omega D u_0 + K u_0 = F \quad (11)$$

, where $u = u_0 e^{i\omega t}$. The undamped system has n eigenvalues ω_i, which satisfy the equation

$$K\hat{u}_i = \omega_i^2 M\hat{u}_i \quad (12)$$

These eigenvectors are orthogonal with respect to M and K. This is shown in Eqs. (13) and (14).

$$\hat{u}_j^T M\hat{u}_i = 0 \qquad i \neq j,\ \omega_i \neq \omega_j \quad (13)$$

$$\hat{u}_j^T K\hat{u}_i = 0 \qquad i \neq j,\ \omega_i \neq \omega_j \quad (14)$$

3.2 Geometry of the crack

As shown in Eq. (3), a crack can be represented mathematically as elastic energy. Therefore, the local flexibility in the presence of the crack can be defined as a function of the geometry of a crack. Figure 2 shows the crack dimensions such as depth, width, and angle.

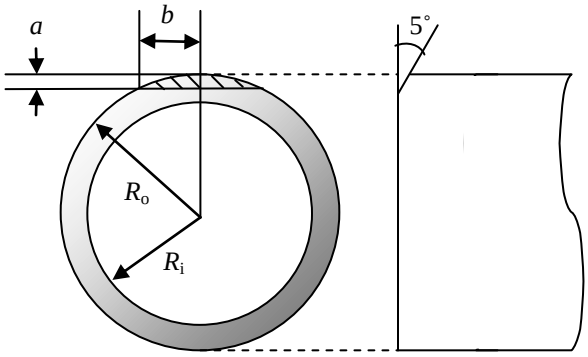

Figure 2. Cross section of the cutaway cracked pipe and the side view.

The effect of the crack geometry and location can be easily investigated by parameterizing the modeling process using COMSOL. In Fig. 2, a = 0.0025 m, b = 0.012 m, and the angle of the crack is 5˚ to the both angles, hence the total cracked angle is 10˚. The location of the crack is placed at the middle of the pipe length.

3.3 Boundary conditions

The Aeroacoustic-Structure Boundary coupling is used to couple an Aeroacoustic model, which only applies to the Linearized Navier-Stokes in Frequency Domain, to the Structural Solid Mechanics component. This

coupling can be used to model fluid structure interaction (FSI) in the frequency domain. The coupling prescribes continuity in the displacement field between two different domains as in Eq. (15).

$$u_{fluid} = i\omega u_{solid} \quad (15)$$

, where u_{fluid} is the fluid velocity and u_{solid} is the solid displacement. This results in the stress being continuous across the boundary between two different domains. This boundary condition will play an important role investigating the effects of the fluid to the vibration mode of the pipe system.

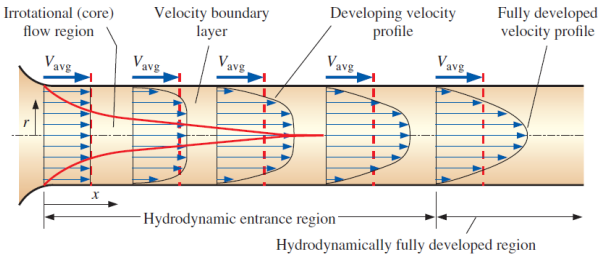

Figure 3. The development of the velocity boundary layer in a pipe [10].

In this paper, we consider the steady, laminar, incompressible flow of fluid with constant properties in the fully developed region of a straight circular pipe. The gravitational effect is negligible. The velocity profile is to be the same at any cross section of the pipe by assuming that flow in pipes is laminar for Re ≤ 2300 and that the flow is fully developed if the pipe is sufficiently long (relative to the entry length). In order to have the entrance effect negligible, each end of the pipe and the fluid sections are chosen as perfectly matched layers (PMLs) as shown in Fig. 1(b). PMLs provide accurate simulations of open pipes and other models with unbounded domains [9]. Figure 3 show the developed average velocity profile which is parabolic in laminar flow. The flow velocity profile is chosen as

$$u(r) = V_{\max}\left[1 - \left(\frac{y^2 + z^2}{R_o{}^2}\right)\right] \quad (16)$$

, where V_{max} is maximum velocity, R_o is the inner pipe radius, y and z are radial distance from the center to each axis (see Fig. 1 for the coordinate system used for the system). Two other assumptions are used for Eq. (16); fluid flow is Newtonian fluid for laminar case, and the no slip condition for the flow on a hard wall inside the pipe. The No slip condition is given in Eq. (17).

$$u = 0 \quad (17)$$

3.4 Mesh and solver

All domains are meshed by sweeping and boundary layers based on Free Triangle elements. They are chosen based on the patch analysis which was performed for both triangle and quadrilateral elements. The analyses show that the result is not sensitive to the type of elements.

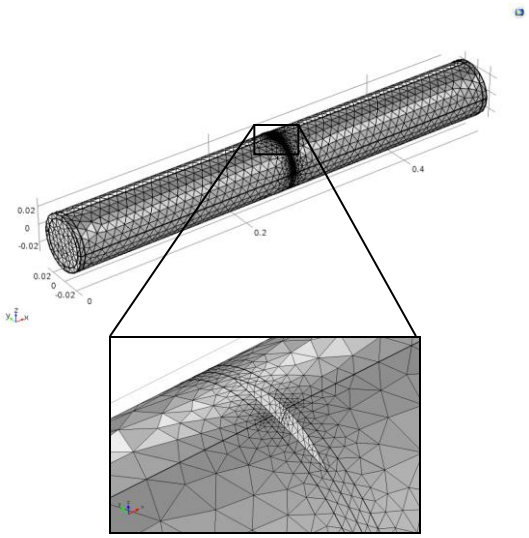

Figure 4. Meshed cracked pipe.

The most vital section to be meshed for this model is the crack itself since it is modeled as relatively small size as shown in Fig. 4. The maximum size is set to 0.2744. This is because it is important to make meshes sufficiently resolved in the acoustic domain. The rule of thumb is that the minimum of ten to twelve degrees of freedom per wavelength are needed for the solution to be reliable with the (default) second-order elements. In the case of acoustic domain, at least five mesh elements per wavelength must be used. Thus, the mesh size depends on the frequencies involved. The numerical value of 0.2744 is used as maximum element size h_{max} which corresponds to 0.2λ, where λ is the wavelength of the sound waves in the acoustic domain. This is because the solutions to acoustics problems are wave like

and the waves are characterized by a wavelength λ which is defined as $\lambda = c/f$ where c is the speed of sound in water and f is frequency. Hence, the wavelength λ has to be resolved by the mesh [11]. Figure 4 show that the zoomed in view of meshed crack.

The model is solved in frequency domain and the solver is chosen for MUMPS.

4. Simulation Results

Numerical simulation yields ideal responses with respect to the fluid loading effect and followed by the influence due to crack to the structure. Varying the speed of the fluid flow inside a pipe, observation is made on its effect to the eigenfrequency.

4.1 Fluid loading and Crack effects

Due to the added mass effect induced by the fluid inside the pipe, a significant reduction in natural frequencies is observed. In Table 2, the comparison of the simulation is made *in vacuo* and with water inside the pipe for only the first natural frequency.

Table 2: Comparison for *in vacuo* and the pipe filled with water for its eigenfrequency

	eigen-frequency	eigenfrequency w/ crack
In vacuo	① 843.56 Hz	② 836.96 Hz
Filled with water	③ 749.63 Hz	④ 747.58 Hz
Percentage decrease	11 %	10 %

The fluid added mass effect is estimated by calculating the frequency reduction ratio δ of each natural frequency defined as

$$\delta = \frac{(f_v - f_w)}{f_v} \qquad (18)$$

where f_v and f_w are the natural frequencies *in vacuo* and with fluid inside the pipe. It can be observed that the eigenfrequency is considerably reduced by the presence of fluid inside the pipe. It also shows that the frequency reduction ratio remains rather similar to each other, which indicates that crack does not influence the frequency reduction ratio.

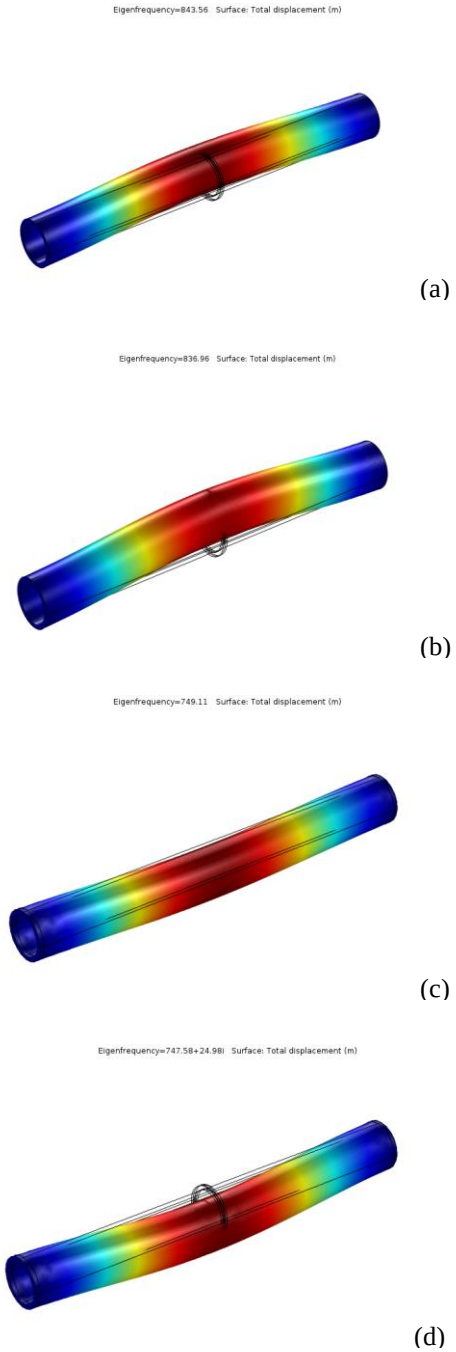

Figure 5. Eigenmodes for the cases in Table 2.

It is important to note that their eigenmodes remain unchanged. This is shown in Fig. 5 where ①, ②, ③, and ④ from Table 2 denote (a), (b), (c), and (d) in Fig. 5, respectively.

4.2 Fluid flow effect

In order to investigate the effect of the velocity of the fluid flow within a pipe with and without crack, frequency analysis has been performed to calculate its eigenfrequency by varying the maximum velocity of the fluid flow. The results have been tabulated in Table 3.

The velocity of the fluid inside the pipe seems to affect the natural frequency of the pipe system such that as the velocity increases, its eigenfrequency decreases. However, there has not been found any specific correlation between them in this work.

Table 3: Comparison for different velocities of the fluid flow inside the pipe for its eigenfrequency

Max. velocity	eigen-frequency	eigenfrequency w/ crack
1 m/s	749.11 Hz	747.58 Hz
10 m/s	702.14 Hz	742.44 Hz

5. Conclusion

In this paper, a pipe conveying fluid flow with crack has been investigated through numerical simulation using COMSOL Multiphysics software. Vibrational behavior of the pipe system has been studied to show the effect of fluid within a pipe as well as that of crack. The obtained results correspond well as expected.

The work to be done in the future would be as follows; (1) investigation of further study of the velocity of the fluid flow in greater detail, (2) investigation of the crack location, (3) study of dual crack effect rather than single crack, and (4) derivation of mathematical model that corresponds with the simulation study.

6. References

1. Dilena, M., Dell'Oste, M. F., and Morassi, A., Detecting cracks in pipes filled with fluid from changes in natural frequencies, *Mechanical Systems and Signal Processing*, **25**, 3186-3197 (2011)
2. Eslami, G., Maleki, V. A., and Rezaee, M., Effect of Open Crack on Vibration Behavior of a Fluid-Conveying Pipe Embedded in a Visco-Elastic Medium, *Latin American Journal of Solids and Structures*, **13**, 136-154 (2016)
3. Petkova, S., and Kisliakov, D., Transverse Earthquake-Induced Vibrations of a Buried Pressure Pipeline Including Fluid-Structure Interaction, *Journal of Theoretical and Applied Mechanics*, **41**, 49-68 (2011)
4. Masoud, A. A., and Al-Said, S., A New Algorithm for Crack Localization in a Rotating Timoshenko Beam, *Journal of Vibration and Control*, **15(10)**, 1541-1561 (2009)
5. Al-Said, S. M., Crack Detection in Stepped Beam Carrying Slowly Moving Mass, *Journal of Vibration and Control*, **14(12)**, 1903-1920 (2008)
6. Al-Said, S. M., Crack identification in a stepped beam carrying a rigid disk, *Journal of Sound and Vibration*, **300**, 863-876 (2007)
7. Al-Said, S. M., and Al-Qaisia, A. A., Influence of Crack Depth and Attached Masses on Beam Natural Frequencies, *International Journal of Modelling and Simulation*, **28(3)**, 239-247 (2008)
8. Son, I., and Yoon, H., Dynamic Stability of Elastically Restrained Cantilever Pipe Conveying Fluid with Crack, *Transactions of KSNVE*, **18(2)**, 177-184 (2008)
9. COMSOL 5.1 Acoustic Module User's Guide.
10. Cengel, Y. A., and Cimbala, J. M., *Fluid Mechanics – fundamentals and Applications 3rd Edition,* 351. McGraw Hill (2010)
11. Lee, J. H., *Bio-Inspired Hydro-Acoustic Sensor for Sensing Directivity of Sound*, Ph.D. Dissertation, University of Washington (2013)

7. Acknowledgements

The authors acknowledge the support of the American University of Sharjah.